Synchrony and Asynchrony of a Neural Population with Spontaneous Leaking and Shunting Inhibitions

Yuliang Shi

Mentor: Charles S. Peskin

Abstract

In this paper we propose a stochastic mathematical model to study a large population of pulse-coupled integrate-and-fire neural oscillators, inspired by the work of R. E. Lee DeVille and Charles S. Peskin [5]. It improves their original model by incorporating spontaneous leaking and inhibitions. This model inherits the bifurcation phenomenon observed in the original model, demonstrate the way that spontaneous leaking contribute to synchronizations, and detect a stronger bifurcation phenomenon under a strong inhibitory feedback loop. Also, we develop mean-field formulations as an approximation to the new model. Numerical results demonstrate that the mean-field approximation capture the main characteristics that observed in the stochastic model, such as bifurcations and feedback-oscillations.

1 Introduction

The study of synchronization phenomenon of non-linear oscillators has brought a wide range of attentions. It is first time introduced by Huygens[10] when studying coupled pendulum clocks. Some review in this field are provided by but not limited to Strogatz [18], Pikovsky et al.[17], Winfree[23].

In this paper, we investigate the synchronization problem under settings of pulse-coupled integrate-and-fire neural oscillators. These oscillators are coupled only when some of them fire. There are two kinds of couplings in our model, namely *excitatory firing* and *inhibitory firing*. Excitatory firing drives the phases of other coupled neurons toward their firing threshold, while inhibition drives their phases away from the threshold.

A lot of work has been done in specific context of these integrate-and-fire oscillators and a wide range of phenomenon has been obsvered and explored (Kuramoto [13][12]; Abbott and van Vreeswijk[1]; Gerstner and van Hemmen[8]; Hansel et al.[9]; Tsodyks et al.[20]; van Vreeswijk et al.[22]; Bressloff and Coombes[2]; Terman et al.[19]; Campbell et al.[3];

Goel and Ermentrout[6]; Lindner et al.[14]). On the other hand, some general but more abstract models have also been explored. Usually, each neuron is represented by a real number $k \in [V_0, V_K]$ as its voltage level. When a neuron's voltage level k been raised to the firing threshold V_K, the corresponding neuron "fires" and is reset to V_0. Knight [11] showed that a population of uncoupled leaky integrate-and-fire neurons can be synchronized by a common periodic input. Peskin [16] has shown that two "slightly leaky" integrate-and-fire oscillator synchronize under reasonable assumptions. A generalization of this result to any number of neurons has been proved by Mirollo and Strogatz [15], who further clarified the role of "leakiness" in synchronization. Moreover, Senn and Urbanczik [21] showed that deterministic networks consisting of nonidentical pulse-coupled oscillators without leakiness synchronize generically. In 2008, DeVille and Peskin [5] showed that a stochastic pulse-coupled neural network with discrete voltage level and without leaking synchronized when couplings are "strong" and it is asynchronous when couplings are "weak". More surprisingly, they further discovered that there exists a range of coupling parameters such that the stochastic model switches spontaneously between synchrony and asynchrony.

In this present paper, we replace the usual deterministic integrate-and-fire neuron by a fully stochastic, continuous-state, leaking, and integrate-and-fire model. Also, we consider neural networks with both excitatory and inhibitory neurons. Although the new model allows complex random network structures, we leave the study of it to future work. We choose to work with a stochastic neuron network for the physiological importance and realistic of synaptic failures and random external inputs. For example, this consideration includes the phenomenon that, with some probability, the arrival of an action potential at a pre-synaptic terminal causes the release of neural transmitters stored in synaptic vesicles. In previous work done by DeVille and Peskin [5], the they investigated a simple case: the number of vesicles released at a given synapse upon the arrival of an action potential is either 0 or 1 and, for each released vesicle, the post-synaptic voltage potential is raised by a same fixed amount. This idealization allowed them to investigate non-leaky excitatory-only neuron populations with discrete states. In order to further investigate the role of leaking and inhibition in synchronization of a fully stochastic neuron population, we need to generalize the old model in a reasonable way, which is not completely straightforward. One possible model of achieving this goal is presented in this paper, and, moreover, we write down a mean-field formulation to approximate the stochastic model.

2 Stochastic Model

In this section we propose a stochastic model based on previous work by R. E. Lee DeVille and Charles S. Peskin [5]. Section 2.1, Section 2.2, and Section 2.3 develop the new model in steps.

Since the role of complex random network structures in synchronization of neurons is out of the scope of our discussion in this paper, we choose one network structure and investigate leaking and inhibitions on this particular network.

2.1 Network Structure for Coupling

Consider a population of pulse-coupled neurons, which are further divided into two subpopulations based on the type of neurotransmitters been released per neuron – inhibitory and excitatory neural populations. Within each of the type of coupling shown (Figure 1), the coupling is from all neurons of the upstream type to all neurons of the downstream type.

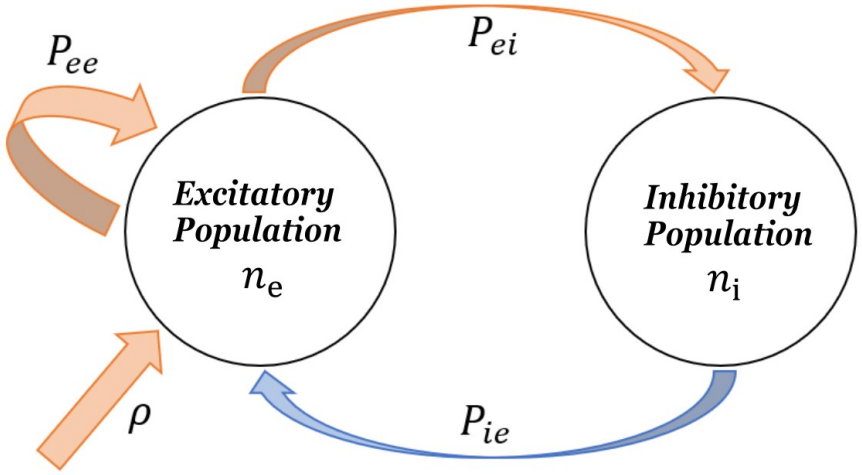

Figure 1: interactions between two subpopulations (inhibitory and excitatory neural populations)

In Figure 1, P_{ee}, P_{ei}, P_{ie} are matrices whose entries are probabilities and ρ is a vector whose entries are probabilities per unit time. $(P_{ee})_{jk}$ is the probability of the k-th excitatory neuron being promoted to higher voltage level by a stochastic jump, if the j-th excitatory neuron fires. Similarly, $(P_{ei})_{jk}$ is the probability of the k-th inhibitory neuron being promoted caused by the j-th excitatory neuron, while $(P_{ie})_{jk}$ is the probability of the k-th excitatory neuron being inhibited if the j-th inhibitory neuron fires. Also, ρ_j is the probability per unit time of the j-th excitatory neuron being promoted because of random external inputs. n_e and n_i are the number of excitatory and inhibitory neurons respectively.

Note that, in the relations explained above, we do not allow an inhibitory neuron to receive any external inputs. Although the network structure that represented by P_{ee}, P_{ei}, P_{ie} can be quite complicated, we restrict our attention to the networks with the same choices for every entries of each of those three matrices. It should be pointed out that this network structure is not an "all-to-all" neural network. For example, inhibitory neurons cannot inhibit themselves and the coupling between neurons are fully stochastic.

In this model, time runs continuously until some neuron has been promoted over firing threshold $V_K \in \mathbb{R}^+$, namely a firing event occurs, and then there may be a cascade of firing events that we model as occurring at an instant of time. We describe the dynamics between

firing cascade first, and the cascade dynamics later.

2.2 Between Firing Cascades

We could define $v_j^e(t) \in [V_0, V_K]$ as the voltage level for the j-th excitatory neuron at time t, where V_K is the threshold for triggering a firing event. Similarly, we could define $v_j^i(t)$. Therefore, vectors $\mathbf{v}^e(t) := (v_j^e(t))_{j=1}^{n_e}$ and $\mathbf{v}^i(t) := (v_j^i(t))_{j=1}^{n_i}$ represents the state of our system at time t, where n_e and n_i are the population size of excitatory and inhibitory neurons.

Spontaneous Promotions by External Inputs: For each excitatory neuron, there is some probability per unit time ρ that it jumps to a higher voltage level as a result of receiving external input. Moreover, the size of the jump, denoted by J, is randomly distributed on the positive real line according to some distribution $\mathbb{D}$. For example, at $\forall t \in \mathbb{R}^+$,

$$v_j^e(t + \Delta t) = min(v_j^e(t) + J, V_K)$$

where

$$\Delta t \sim exp(\rho) \quad \text{and} \quad J \sim \mathbb{D} \equiv gamma(a, b)\ (a, b > 0)$$

and Δt is waiting time until the j-th neuron jumps. The fact that $\mathbb{D}$ is a continuous one is crucial to the formulations shown in Section 3, which will be explained in Section 3.1.

Leaking Voltage: The leaking process happens only between firing cascades: voltage level of a neuron leak exponentially towards the zero voltage level. With spontaneous promotions and leaking, we conclude what happens between firing cascades as follows

$$\frac{dv_j^e}{dt} = -\gamma v_j^e + \sum_i \delta(t_i) J_i \quad \text{and} \quad \frac{dv_j^i}{dt} = -\gamma v_j^i$$

where

$$\Delta t_i \sim exp(\rho),\ \Delta t_i = t_i - t_{i-1},\ \text{and}\ J_i \sim \mathbb{D}$$

as long as the voltage level of the j-th neuron is below firing threshold V_K. Note that all the J_i above are caused by external inputs, and in the particular network structure we restricted our attention to, as in Figure 1, the inhibitory neurons do not receive external inputs. We say that $\gamma \in \mathbb{R}^+$ is the rate of leaking in later discussions.

2.3 Firing Cascade

When the voltage level of some excitatory neuron has been promoted above the firing threshold K, the system enters a firing cascade, i.e. a sequence of contiguous firings in which each one caused by some previous firing. We assume such a cascade happens in an instance of time and that each neuron can only fire once in each cascade. Every neuron that fires during a cascade has the possibility of influencing other neurons, and some of these may fire. We model this by creating a queue of neurons that have fired but whose influence has not yet been taken into account. The cascade ends when the queue is empty. During a firing

cascade, there is no leaking process, since no time has elapsed. At the end of a cascade, all of the neurons that fired are reset to the zero voltage level.

An Excitatory Firing: If an excitatory neuron fires, there is certain probability that another neuron been promoted by a stochastic jump. For simplicity, we choose the same distribution for stochastic jumps caused by excitatory firings as for spontaneous input.

An Inhibitory Firing: If an inhibitory neuron fires, only excitatory neurons can receive the signal in our model. The inhibition we are considering here is shunting inhibition. If a neuron is inhibited, then its voltage level decays to a fixed fraction of its previous value.

3 Mean-Field Approximations

In this section, we do a mean-field approximation to the stochastic system described above. In section 3.1, we define basic quantities that the mean-field approximation focuses on. In section 3.2, a derivation of the mean-field formulation is presented. In section B, a discrete version of the mean-field formulation is established based on the continuous one. In Appendix A, a detailed mean-field algorithm is stated.

3.1 Preliminaries

In the stochastic model, we denote $\mathbb{P}$ as the corresponding stochastic process without further specifying the underlying probability space. With those notations established above, the state of our system at time t could be fully described if, for any $k_1, k_2 \in (0, K)$, the value of following random variables are known:

$$\mathbb{M}^e(k_1, k_2, t) := \Sigma_{j=1}^{n_e} \mathcal{X}_{\{v_j^e(t) \in [k_1, k_2]\}}$$

$$\mathbb{M}^i(k_1, k_2, t) := \Sigma_{j=1}^{n_i} \mathcal{X}_{\{v_j^i(t) \in [k_1, k_2]\}}$$

$$\mathbb{N}_0^e(t) := \Sigma_{j=1}^{n_e} \mathcal{X}_{\{v_j^e(t)=0\}}$$

$$\mathbb{N}_K^i(t) := \Sigma_{j=1}^{n_i} \mathcal{X}_{\{v_j^i(t)=K\}}.$$

where $\mathcal{X}_A$ is indicator function of event A. $\mathbb{M}^e(k_1, k_2, t)$ and $\mathbb{M}^i(k_1, k_2, t)$ are the numbers of excitatory and inhibitory neurons sitting between voltage level k_1 and k_2 at time t respectively. It does not make sense to talk about "number density" of neurons at voltage level k in the stochastic model. However, we could make sense of this number density notions in mean-field limits. Define functions $X_e(k, t)$: $(0, K) \times [0, \infty) \to \mathbb{R}^+$ and $X_i(k, t)$: $(0, K) \times [0, \infty) \to \mathbb{R}^+$ such that for any interval $[k_1, k_2] \in (0, K)$ we have

$$\int_{k_1}^{k_2} X_e(k, t)dk := \mathbb{E}_{\mathbb{P}}[\mathbb{M}^e(k_1, k_2, t)]$$

$$\int_{k_1}^{k_2} X_i(k, t)dk := \mathbb{E}_{\mathbb{P}}[\mathbb{M}^i(k_1, k_2, t)]$$

representing number density of excitatory and inhibitory neurons on level k at time t respectively.

Moreover, by considering the stochastic model, we notice that after each firing cascade there will be some number of neurons being reset to the zero voltage level. Also, between firing cascade, there will be a process which accumulates neurons at the topmost level in order to trigger a firing event. The fact that the jumping distribution $\mathbb{D}$ is continuous guarantees that all the voltage level except the zero and topmost level will not have concentrations. For those reasons, a concentration of neurons will only be sitting at the lowest and the topmost level, i.e. the zero level and firing threshold K. One could also interpret those two quantities as two δ functions and incorporate them into X_e and X_i. For the purpose of simplicity, we consider them separately from X_e and X_i and define functions $N_0^e(t) : [0, \infty) \to [0, n_e]$ and $N_K^e(t) : [0, \infty) \to [0, n_e]$ as

$$N_0^e(t) := \mathbb{E}_{\mathbb{P}}[\mathbb{N}_0^e(t)]$$
$$N_K^e(t) := \mathbb{E}_{\mathbb{P}}[\mathbb{N}_K^e(t)].$$

These two functions represents the average number of excitatory neurons on the zero and the topmost voltage level at time t respectively. Similarly, we define random variables $\mathbb{N}_0^i(t)$ and $\mathbb{N}_K^i(t)$ for inhibitory neurons as well as their mean-field limits $N_0^i(t)$ and $N_K^i(t)$.

The firing condition can be approximated by

$$N_K^e(t) \geq 1,$$

which is one the places where approximations come into play. Let $t_0 = 0$ and define t_n for $n \in \{1, 2, ...\}$ recursively as

$$t_n = \inf\{t_{n-1} + \Delta t : N_K^e(t_{n-1} + \Delta t) \geq 1 \text{ and } \Delta t > 0\}$$

which represents time of the n-th firing cascade. A convention we are following is $X_e(k, t_n)$, $X_i(k, t_n)$, $N_K^e(t_n)$, and $N_K^i(t_n)$ represent the corresponding values at the end of the n-th firing cascade.

3.2 Derivations

There are more than one approach to reveal the final formulations and we only discuss one of them as presented in the following Sections. An assumption that holds for all later computations is that $N_K^e(t)$ and $N_K^i(t)$ will not have exponential leaking toward zeros level at any time.

3.2.1 Between Firing Cascades

First, we write down a formula for flux of the excitatory neuron population and assuming that up-crossing flux through level k is positive:

$$F_e(k, t) := -\gamma k X_e(k, t) + \rho N_0^e(t)\mathbb{P}(J \geq k) + \int_0^k \rho X_e(\epsilon, t)\mathbb{P}(J \geq k - \epsilon)d\epsilon, 0 < k < K \quad (1)$$
where $J \sim \mathbb{D}$ with density $f_J(x)$.

Then, we write down dynamics for the number of neurons over an interval $[k_1, k_2]$, with $0 < k_1 < k_2 < K$.

$$\frac{d}{dt}\Big(\int_{k_1}^{k_2} X_i(k,t)dk\Big) = \gamma k_2 X_i(k_1,t) - \gamma k_1 X_i(k_2,t) \tag{2}$$

$$\begin{aligned}\frac{d}{dt}\Big(\int_{k_1}^{k_2} X_e(k,t)dk\Big) &= F_e(k_1,t) - F_e(k_2,t) \\ &= \Big(-\gamma k_1 X_e(k_1,t) + \rho N_0^e(t)\mathbb{P}(J \geq k_1) + \int_{-\infty}^{k_1} \rho X_e(\epsilon,t)\mathbb{P}(J \geq k_1 - \epsilon)d\epsilon\Big) \\ &\quad - \Big(-\gamma k_2 X_e(k_2,t) + \rho N_0^e(t)\mathbb{P}(J \geq k_2) + \int_{-\infty}^{k_2} \rho X_e(\epsilon,t)\mathbb{P}(J \geq k_2 - \epsilon)d\epsilon\Big)\end{aligned} \tag{3}$$

Note that, since the inhibitory neurons in our model does not receive external inputs, there are no such terms corresponding to spontaneous promotions and thus only the leaking terms left. The dynamics of $N_0^e(t)$ and $N_K^e(t)$ can be easily write down, while $N_0^i(t)$ and $N_K^i(t)$ do not change between cascade since there are no leaking and external inputs to them. From equations (2)-(3) and with enough regularity assumptions on X_e and X_i, we arrive at the following conclusions:

$$\frac{d}{dt}N_0^e(t) = -\rho N_0^e(t) \tag{4}$$

$$\frac{d}{dt}N_K^e(t) = \int_0^K \rho X_e(\epsilon,t)\mathbb{P}(J \geq K - \epsilon)d\epsilon + \rho N_0^e(t)\mathbb{P}(J \geq K) \tag{5}$$

$$\frac{\partial}{\partial t}X_e(k,t) = \gamma\frac{\partial}{\partial k}\Big(kX_e(k,t)\Big) - \rho X_e(k,t) + \rho N_0^e(t) f_J(k) + \int_0^k \rho X_e(\epsilon,t) f_J(k-\epsilon)d\epsilon \tag{6}$$

$$\frac{d}{dt}N_0^i(t) = 0 \tag{7}$$

$$\frac{d}{dt}N_K^i(t) = 0 \tag{8}$$

$$\frac{\partial}{\partial t}X_i(k,t) = \gamma\frac{\partial}{\partial k}\Big(kX_i(k,t)\Big) \tag{9}$$

Equations (4)-(5) and (7)-(9) provide complete descriptions of dynamics for mean-field limits of the stochastic systems when it is between cascades. It could be checked analytically that either (4)-(5) or (7)-(9) are conservative of the total number of neurons, i.e.

$$\int_0^K \frac{\partial}{\partial t}X_e(k,t)dk + \frac{d}{dt}N_0^e(t) + \frac{d}{dt}N_K^e(t) = 0 \tag{10}$$

$$\int_0^K \frac{\partial}{\partial t}X_i(k,t)dk + \frac{d}{dt}N_0^i(t) + \frac{d}{dt}N_K^i(t) = 0 \tag{11}$$

3.2.2 An Excitatory Firing Within a Cascade

We start from here to the end of Section 3.2.3, discussing how those mean-field limits being updated inside a firing cascade, which happens at a instant of time. We proceed as before

by considering flux caused by an excitatory firing. Assume that up-crossing voltage level k is positive, then

$$F_{cas}(k) := \int_0^k pX(\epsilon, t)\mathbb{P}(J \geq k - \epsilon)d\epsilon + pN_0(t)\mathbb{P}(J \geq k) \tag{12}$$

Let X_{old} denote either the number density of excitatory or inhibitory neurons before one firing event occurs and X_{new} denote the resulting density after a firing event. Therefore, we have the following result on a interval $[k_1, k_2]$, with $0 < k_1 < k_2 < K$:

$$\int_{k_1}^{k_2} X_{new}(k, t) - X_{old}(k, t)dk = F_{cas}(k_2) - F_{cas}(k_1) \tag{13}$$

$$\Rightarrow \frac{1}{k_2 - k_1}\int_{k_1}^{k_2} X_{new}(k, t)dk = \frac{1}{k_2 - k_1}\int_{k_1}^{k_2} X_{old}(k, t)dk - \frac{F_{cas}(k_2) - F_{cas}(k_1)}{k_2 - k_1} \tag{14}$$

Let $k_2 \to k_1$, and with some regularity assumptions over X_{old} and X_{new}, we have

$$X_{new} = (1 - p)X_{old}(k, t) + \int_0^k pX_{old}(\epsilon, t)f_J(k - \epsilon)d\epsilon + pN_0(t)f_J(k), \tag{15}$$

Equation (15) provides us with the updating rule for number density of neurons of each type after an excitatory firing occurs. To make later discussion easier, we define the following two operators:

$$G_{ee}(X, N_0)(k, t) := (1 - p_{ee})X(k, t) + \int_0^k p_{ee}X(\epsilon, t)f_J(k - \epsilon)d\epsilon + p_{ee}N_0(t)f_J(k) \tag{16}$$

$$G_{ei}(X, N_0)(k, t) := (1 - p_{ei})X(k, t) + \int_0^k p_{ei}X(\epsilon, t)f_J(k - \epsilon)d\epsilon + p_{ei}N_0(t)f_J(k) \tag{17}$$

Therefore, we conclude the updating scheme after an excitatory firing within a cascade as (18)-(19) and (20)-(21) for excitatory population and inhibitory population repectively:

$$N_0^e \leftarrow (1 - p_{ee})N_0^e, \;\; X_e \leftarrow G_{ee}(X_e, N_0^e) \tag{18}$$

$$N_K^e \leftarrow N_K^e + \int_0^K p_{ee}X_e(\epsilon, t)\mathbb{P}(J \geq K - \epsilon)d\epsilon + p_{ee}N_0^e(t)\mathbb{P}(J \geq K) \tag{19}$$

$$N_0^i \leftarrow (1 - p_{ei})N_0^i, \;\; X_i \leftarrow G_{ei}(X_i, N_0^i) \tag{20}$$

$$N_K^i \leftarrow N_K^i + \int_0^K p_{ei}X_i(\epsilon, t)\mathbb{P}(J \geq K - \epsilon)d\epsilon + p_{ei}N_0^i(t)\mathbb{P}(J \geq K) \tag{21}$$

3.2.3 An Inhibitory Firing Within a Cascade

As shown in our network structure (Figure 1), an inhibitory firing can only influence excitatory neurons with probability p_{ie}, while an inhibitory neuron are not allowed to inhibit itself. And once a excitatory neuron being inhibited, its voltage level decays to some fix

fraction q of current voltage level. Similarly, the operator could be defined as:

$$X_{new}(k,t) = G_{ie}(X_{old})(k,t) := \begin{cases} X_{old}(k,t) - p_{ie}X_{old}(k,t) + p_{ie}X_{old}(\frac{k}{q},t), \text{ if } \frac{k}{q} \leq K \\ X_{old}(k,t) - p_{ie}X_{old}(k,t), \text{ otherwise} \end{cases} \tag{22}$$

At the same time, all the other mean-field quantities stay unchanged. Therefore, the above is a complete updating scheme after a single inhibitory firing event.

3.2.4 Exiting Criterion for a Firing Cascade

At time t_n, the system enters into the n-th firing cascade, at the start of which we initialize a queue Q to store neurons that reach the firing threshold but have not yet been taken into account. By iterating through Q, we will be able to update the mean-field quantities by a sequence of updating schemes determined by the type of the current firing neuron. At the same time Q is extended by new neurons that being promoted to threshold K. We say that a cascade stops at iteration τ if and only if

$$\tau = \inf\{m \in \mathbb{Z}^+ : |Q| = 0\}$$

where $|Q|$ is the size of the queue Q.

At each iteration, we remove the first neuron in Q and calculate $\Delta l_e = \lfloor N_K^{e,new} - N_K^{e,old} \rfloor$ and $\Delta l_i = \lfloor N_K^{i,new} - N_K^{i,old} \rfloor$. Then, initialize a list of Δl_e 1's and Δl_i 0's, randomly permute it, and extend Q at the end with this new list.

4 Results

4.1 Bifurcations Between Synchrony and Asynchrony

In Deville and Peskin[5]'s model, they not only observed synchronized firings under strong coupling and asynchronized firings under weak couplings, but also discovered a bi-stable phenomenon within a range of coupling parameters. That is the phase transition between synchronized modes and asynchronized modes happens not at a critical point but at a critical range of coupling parameters, within which there is bifurcation phenomenon and allowing the stochastic model switching spontaneously between synchrony and asynchrony. Evidencing by the results shown below, we claim that both the stochastic model and the mean field approximations that we proposed earlier captures synchronization, asynchronization, and bifurcations. In this section, we restrict our attention to the simplest case where both leaking and inhibitions are zero.

Figure 1 includes snapshots from a phase transition start at a asynchronized state while end up to a synchronized state, during which we observe the bifurcation phenomenon. As in the middle sub-figure, when we have $p_{ee} = 0.0100$, we could observe the state switches back and force and the waiting time for switching seems have its own randomness built into it. We conjectured that the waiting time is exponentially distributed and we are planning

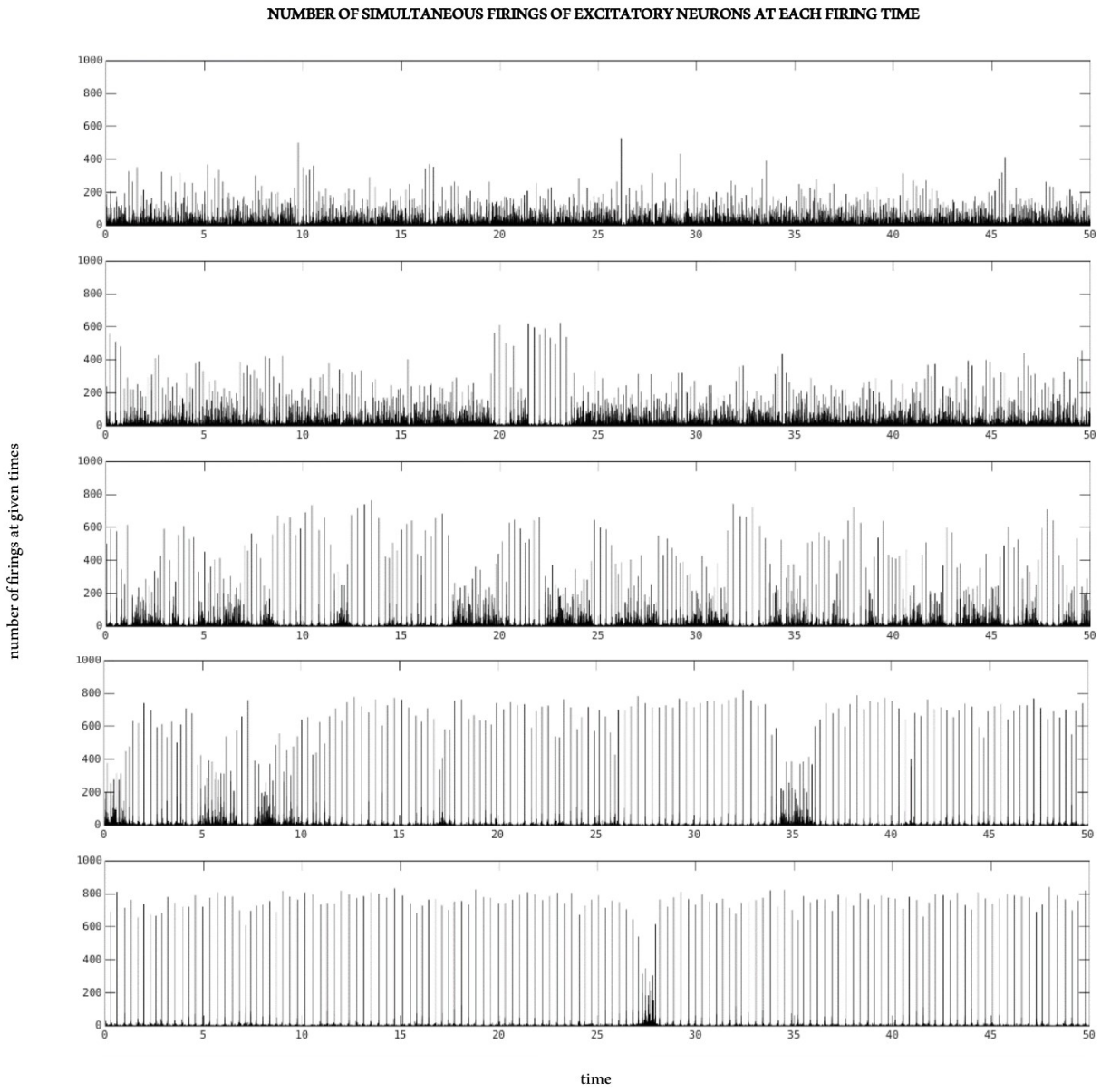

Fig. 1: Stochastic Neural Network Model, Without Leakage and Inhibitions

†The set of experiments presented above are under common parameter choices: $n_e = 1000$, $K = 10$, $\gamma = 0$, $n_i = 0$, $\rho = 10$. And from top to bottom, we have $p_{ee} = 0.0096$, $p_{ee} = 0.0098$, $p_{ee} = 0.0100$, $p_{ee} = 0.0102$, $p_{ee} = 0.0104$. We choose the jump distribution $\mathbb{D}$ as *Gamma* distribution with mean 1 and variance 0.25. Note that these are results come out of the stochastic model explained in Section 2.

to show this directly in future work. In this simplest case, we could actually predict around which value of p_{ee} we will have this phase transition using some non-rigorous calculations. Assume we are at a totally asynchronized state and a cascade happens, the condition for

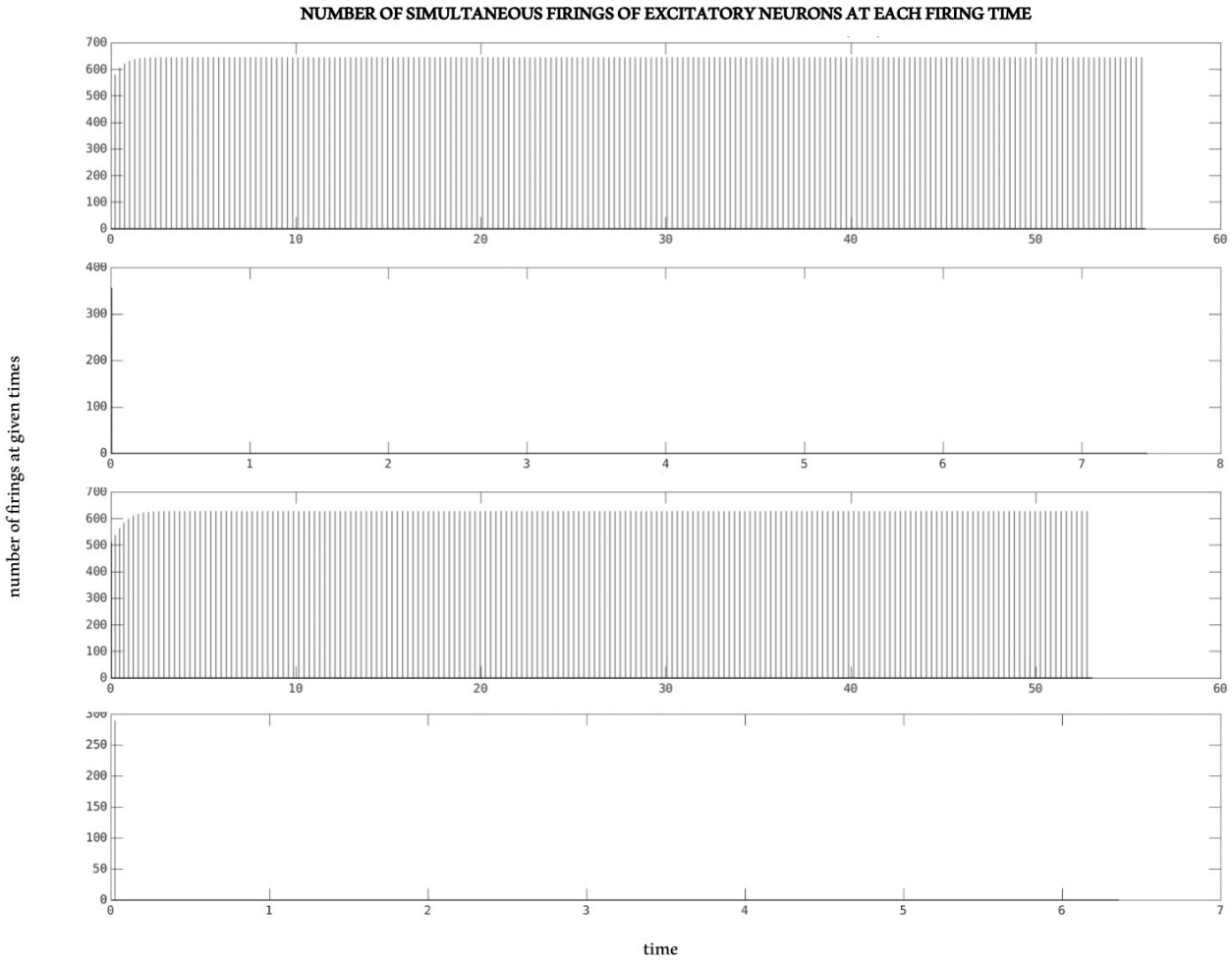

Fig. 2: Mean-Field Approximations, Without Leakage and Inhibitions

†The set of experiments presented above are under common parameter choices (same as Figure 1): $n_e = 1000$, $K = 10$, $\gamma = 0$, $n_i = 0$, $\rho = 10$. Also, the number of discrete voltage level $d = 200$. The first two plots have $p_{ee} = 0.0102$, while the other two have $p_{ee} = 0.0103$. Again, we choose the jump distribution $\mathbb{D}$ as *Gamma* distribution with mean 1 and variance 0.25. In other word, the first two plots sharing exactly the same parameter choice but with different randomized initial condition. The same situations happens to the other two plots. Note that these are results come out of the deterministic mean-field model explained in Section 3 and Appendix C.

only one neuron fires in this cascade is $p_{ee}\frac{n_e}{K} < 1$ if we assume that neurons are distributed roughly uniformly on discrete voltage level $\{0, 1, ..., K-1\}$. The reason we could think of this as discrete voltage level out a continuum $[0, K]$ is that, in the experiments above, we choose the jump distribution $\mathbb{D}$ with mean 1 and small variance. In this case $p_{ee}\frac{n_e}{K} < 1$ implies that $p_{ee} = 0.01$ since we have $n_e = 1000$ and $K = 10$.

Parallel to our discussions of the stochastic model, the mean-field approximation actually

captures those phenomenon that mentioned above in a slightly different flavor. In Figure 2, we have four snapshots from the bifurcation range under the same choices for n_e, K, γ, n_i, ρ, and $\mathbb{D}$ as above. In first two plots, by randomly initialize the starting value of X_E and X_I, we get two completely different modes with $p_{ee} = 0.0102$. Similarly, we also get two different modes with $p_{ee} = 0.0103$. Since each mode corresponding to a steady state of the mean-field system, we again observed the bi-stable phenomenon but in a deterministic system. The fact that those results in Figure 1 comes from a stochastic system makes them noisy but ensure they are capable of switching back and force spontaneously. Moreover, if we compare the size of bursts in corresponding plots of Figure 1 and 2, we could see that they match each other pretty well within the synchronized scheme.

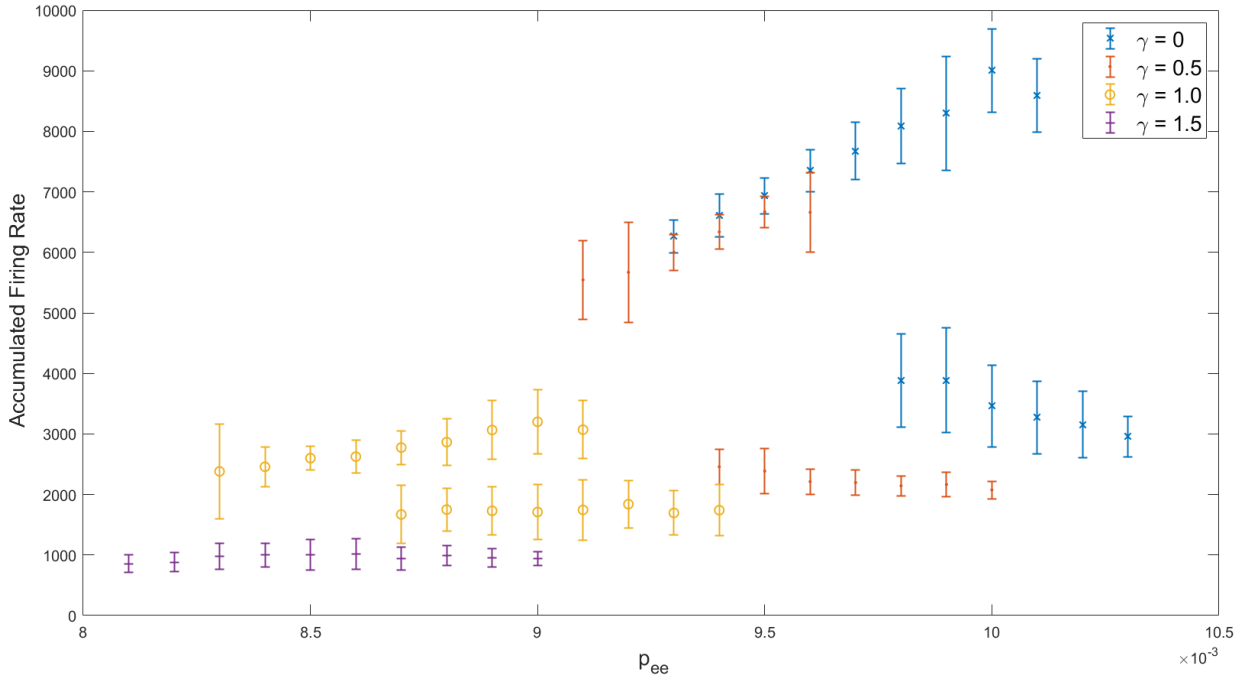

Fig. 3: Leaking and Bifurcations, Without Inhibitions

†The set of experiments presented above are under common parameter choices: $n_e = 1000$, $K = 10$, $n_i = 0$, $\rho = 10$. We change p_{ee} and γ and calculate the accumulated firing rate in each possible mode under every set of parameters. Note that these are results come out of the stochastic model explained in Section 2.

4.2 Leaking Contributes to Synchronizations

In this Section, we focus on results related to spontaneous leaking, remove inhibitory neurons for now, and study how leaking affects the range of bifurcations. In Figure 3, we

could see that as γ increases, the bifurcation range shifts to lower value, which indicates that leaking is makes the phase transition from asynchronous to synchronous happens at a weaker coupling condition. At the same time, the difference between accumulated firing rate of those two modes is driven towards each other when leaking rate γ is large, and such difference eventually becomes indistinguishable.

In particular, three snapshots shown in Figure 4 illustrate the contribution of leaking towards synchronized phase at a specific p_{ee} value. Fixing all other parameters unchanged, by taking leaking rate $\gamma = 0.5, 1.0, 1.5$ from the topmost plot to the bottom one, we observe that the stochastic system changes from an asynchronous mode to a synchronized one.

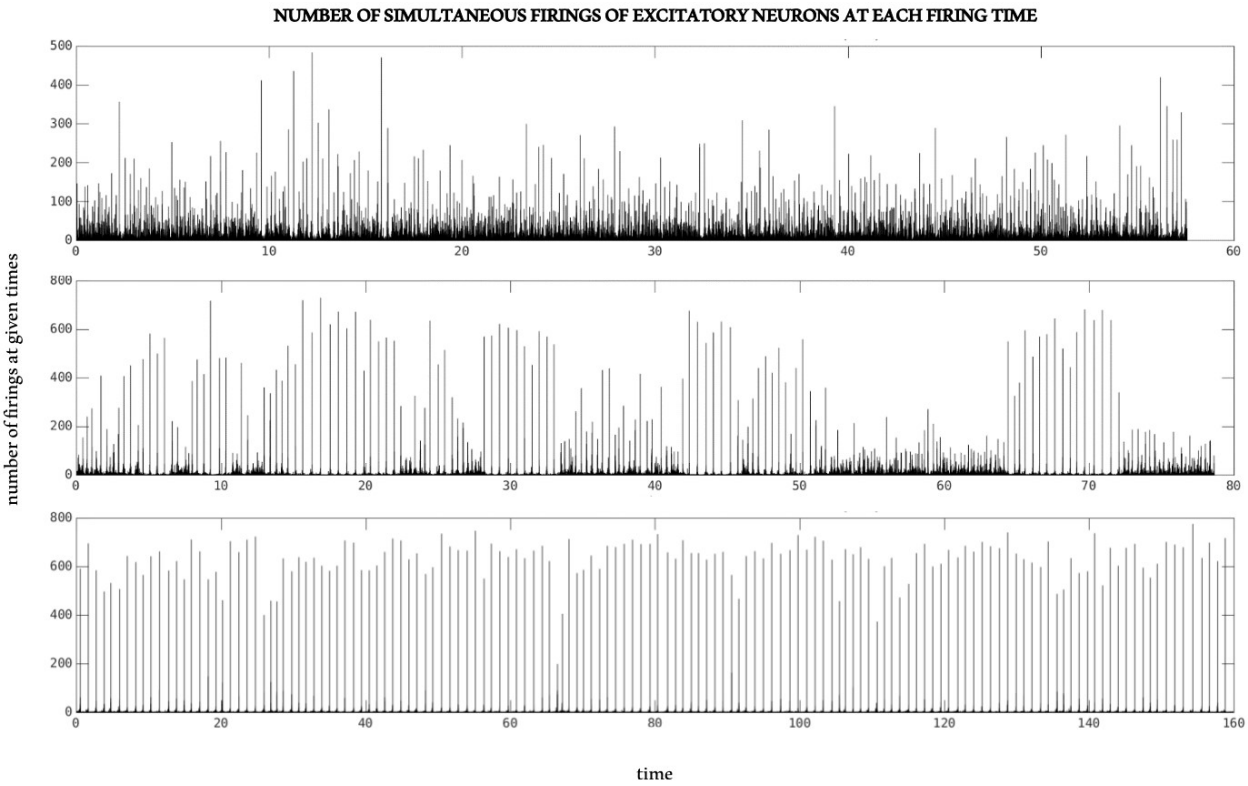

Fig. 4: Leaking and Bifurcation with $p_{ee} = 0.0094$, Without Inhibitions

†The set of experiments presented above are under common parameter choices: $n_e = 1000$, $K = 10$, $n_i = 0$, $\rho = 10$. And from top to bottom, we have $\gamma = 0.5$, $\gamma = 1.0$, $\gamma = 1.5$. We choose the jump distribution $\mathbb{D}$ as *Gamma* distribution with mean 1 and variance 0.25. Note that these are results come out of the stochastic model explained in Section 2.

4.3 Feedback Oscillations Caused by Inhibitory Populations

In this section, we are interested in the phenomenon of feedback oscillations under a strong inhibition-feedback loop. That is neural populations are switching between synchronized modes and asynchronized modes because of a negative feedback loop caused by

inhibitions. An example of it is shown by Figure 5.

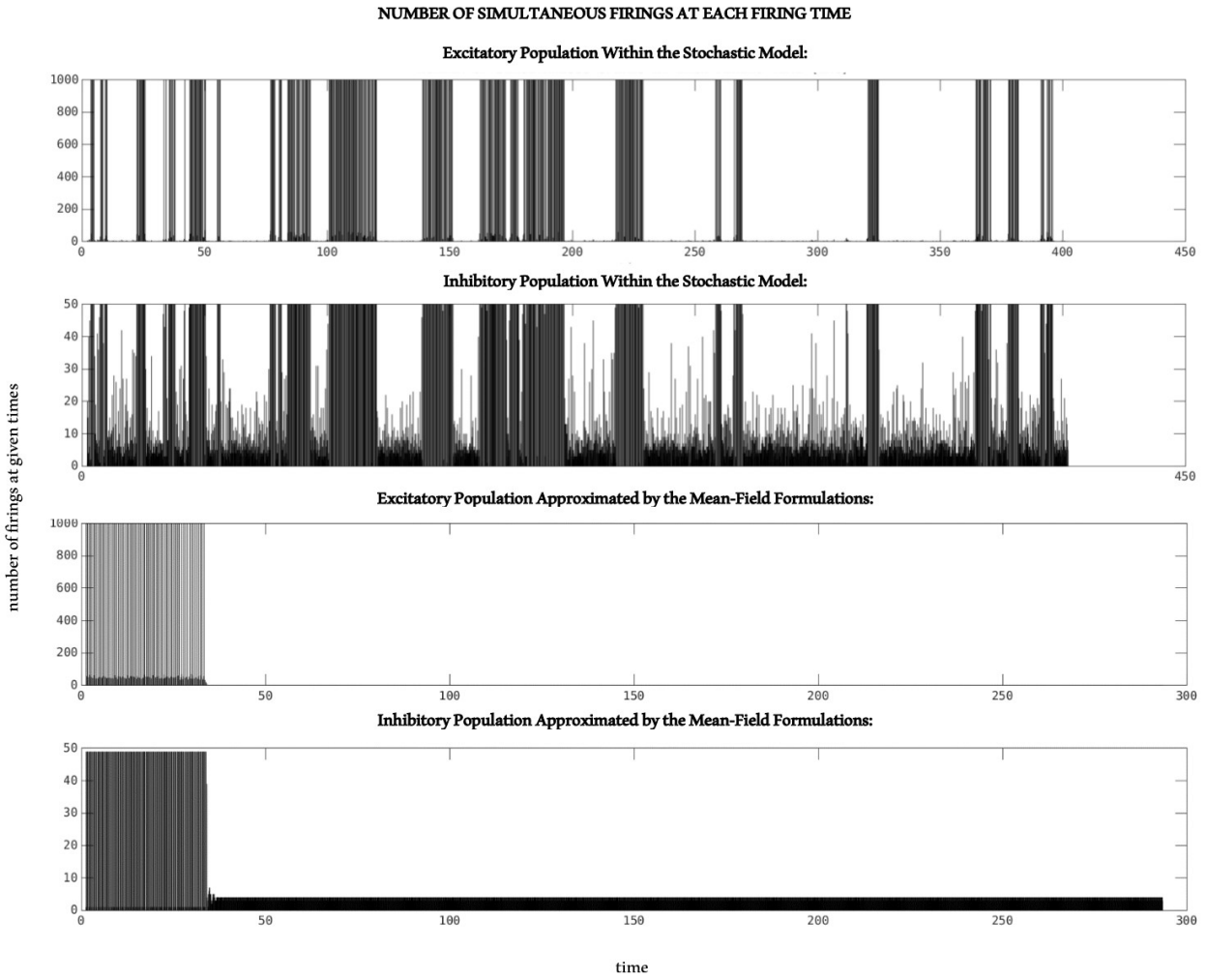

Fig. 5: Feedback Oscillations

†There are three experiments and each of them has two plots, one to the excitatory neurons (EXC) and one for inhibitory neurons (IHB). They all have the same parameter choices but are results from Stochastic (first 2 plots) and Mean-Field models (the other 2 plots). The parameter choices are $n_e = 1000$, $K = 10$, $n_i = 50$, $p_{ee} = 0.2$, $p_{ie} = 0.8$, $p_{ei} = 0.8$, $\rho = 10$. We choose the jump distribution $\mathbb{D}$ as *Gamma* distribution with mean 1 and variance 0.25.

We see that, in the stochastic system, there are two modes - Synchronous and Asynchronous modes. Similar to Section 4.1 and Section 4.2, under strong inhibition feedback loop, we have a bifurcation phenomenon that allow the stochastic system switching between those two modes. However, the mean-field deterministic system shows that the underline steady states arein different situation. In the last 2 plots in Figure 5, the early phase corresponding to the synchronized mode while the later phase corresponding to the asyn-

chronous mode. After running many other experiments with different initial conditions, the mean field system always experience similar situation as Figure 5: staring with the unstable steady state (synchrony) and ending in a stable and absorbing steady state (asynchrony).

5 Conclusion

This paper proposes a fully stochastic model to simulate an neuron network, which allows complex network structures, leaking and inhibitions. Based on this model, we explore the role of leaking and shunting inhibitions in terms of synchronization of stochastic neural network and continue to observe bifurcation phenomenon within a range of parameter choices. Our results evidence that leaking contributes positively to synchronization of neural populations and stronger leaking makes synchronization and asynchronization states less distinguishable form the accumulative firing rate. Within a range of parameter choices, shunting inhibitions result in a bifurcation phenomenon because of the negative feedback-loop which makes the model oscillates between synchrony and asynchrony. Comparing to the bifurcations in section 4.1, this new bifurcation phenomenon caused by the feedback loop works for wider range of parameters and has more distinguishable switching between synchronous and asynchronous states.

To analysis this model, we also propose a mean-field approximation to the stochastic model. By numerically solving this mean-field systems, we have cleaner views over the steady states within the range of bifurcations. In particular, we know that both synchronous and asynchronous states are stable when only having coupled excitatory population. However, the underlying synchronous state is less stable when having the negative feedback loop, while the asynchronous state is stable and absorbing. In future work, we are also aiming at searching for rigorous mathematical relations between the stochastic model and the mean-field system.

6 Acknowledgement

I would like to show my gratitude to my mentor, Professor Charles S. Peskin, for his great guidance and encouragement. It is his wisdom that kept me on the right track and lighted up paths through darkness. I would also like to present my special thanks to Dr. Charles Puelz and Robert Webber for assisting me with the projects and organizing A.M.S.U.R.E weekly groups meetings. I want to thank Professors Aleksandar Donev for helping me to improve the overall presentation of my research outcomes. Also, I want to express my thanks to Professor Miranda Holmes-Cerfo for leading and supporting the undergraduate research program. Finally, I would like to thank NYU Math Department for funding this research.

A Pesudo-Code of Stochastic Model

Algorithm 1 Simulating Neural Networks with Leaking and Shunting Inhibitions

$t \leftarrow 0$
for $j \in \{1, ..., n\}$ **do**
  choose $v_j \in [0, K)$
end for
$type(1 : n_e) \leftarrow 0$, $type(n_e + 1 : n_e + n_i) \leftarrow 1$
while $t < t_{max}$ **do**
  choose j uniformly in $\{1, ..., n\}$
  $v_j \leftarrow v_j + J$, where $J \sim \mathbb{D}$
  if $v_j \geq K$ **then**
    $Q \leftarrow [j]$
    while $|Q| > 0$ **do**
      $c \leftarrow Q(1)$, $newlist \leftarrow [\,]$, $Q \leftarrow Q(2 : end)$, $\tau = type(c)$
      for $k \in \{1, ..., n\}$ **do**
        if $v_k < K$ **then**
          if $rand < p_{c,k}$ **then**
            if $\tau == 1$ **then**
              $v_k \leftarrow v_k + J$, where $J \sim \mathbb{D}$
              if $v_k \geq K$ **then**
                append k to $newlist$
              end if
            else
              $v_k \leftarrow v_k * q$
            end if
          end if
        end if
      end for
      $Q \leftarrow [Q, \text{randperm}(newlist)]$
    end while
  end if
  $v_j \leftarrow 0$ if j-th neuron just fired
  $t \leftarrow t + \tau$, where $\tau \sim exp(N\rho)$
end while

B Discretization of the Mean-Field Formulations

In this section we describe a discrete version of Mean-Field Formulations for mainly three purposes. First, this discrete version derives from the continuous one discussed above and serves as a numerical scheme to implement it. Second, it is a direct comparison with various models consist of discrete voltage levels introduced by Deville and Peskin [5], Deville and Yi Zeng [4], Georgiadis and Sornette [7]. Third, by doing matrix analysis on this discrete model, we will have a tool to understand the continuous one. In this section, we will derive the model from the continuous formulation. For a detailed description of the algorithm, please referring to Appendix C.

Define $X_E(t), X_I(t) : [0,\infty) \to \mathbb{R}^{+(d+2)}$ as state vectors with $\|X_E\|_{l_1}(t) = n_e$ and $\|X_I\|_{l_1}(t) = n_i$ for any time t, which comes from discretizing $[0, K]$ into d mesh intervals. That is

$$X_E^l(t) = \begin{cases} N_0^e(t), & l = d \\ N_K^e(t), & l = d+1 \\ \int_{(l-1)\frac{K}{d}}^{l\frac{K}{d}} X_e(k,t)dk, & 0 \le l \le d-1, \end{cases} \tag{23}$$

$$X_I^l(t) = \begin{cases} N_0^i, & l = d \\ N_K^i(t), & l = d+1 \\ \int_{(l-1)\frac{K}{d}}^{l\frac{K}{d}} X_i(k,t)dk, & 0 \le l \le d-1. \end{cases} \tag{24}$$

Consider the time is between two firing cascades, by discretizing equations (4)-(9) we could write down dynamics for state vectors X_E

$$\frac{\mathbf{d}}{\mathbf{d}t}X_E^d = -\rho X_E^d \tag{25}$$

$$\frac{\mathbf{d}}{\mathbf{d}t}X_E^{d-1} = \gamma d X_E^{d-1} - \rho X_E^{d-1} \tag{26}$$

$$\frac{\mathbf{d}}{\mathbf{d}t}X_E^l = \gamma(l+1)X_E^{l+1} - \gamma l X_E^l - \rho X_E^l + \rho\mathbb{P}\Big[l\frac{K}{d} \le J \le (l+1)\frac{K}{d}\Big]X_E^d \tag{27}$$
$$+ \sum_{m=0}^{l} \rho\mathbb{P}\Big[(l-m)\frac{K}{d} \le J \le (l-m+1)\frac{K}{d}\Big]X_E^m, \;\; 0 \le l \le d-2$$

$$\frac{\mathbf{d}}{\mathbf{d}t}X_E^{d+1} = \rho\mathbb{P}\Big[J \ge K\Big]X_E^d + \sum_{l=1}^{d-1} \rho\mathbb{P}\Big[J \ge K - l\frac{K}{d}\Big]X_E^d \tag{28}$$

And similarly for vector X_I, we write

$$\frac{\mathbf{d}}{\mathbf{d}t}X_I^d = 0, \frac{\mathbf{d}}{\mathbf{d}t}X_I^{d+1} = 0 \tag{29}$$

$$\frac{\mathbf{d}}{\mathbf{d}t}X_I^{d-1} = \gamma d X_I^{d-1} \tag{30}$$

$$\frac{\mathbf{d}}{\mathbf{d}t}X_I^l = \gamma(l+1)X_I^{l+1} - \gamma l X_I^l, \;\; 0 \le l \le d-2 \tag{31}$$

And the solutions to (25)-(28) and (29)-(31) are $X_E(t) = X_E(0)e^{Et}$ and $X_I(t) = X_I(0)e^{It}$, where E and I are corresponding matrix to the ODE's. Then, consider the moment when the system is within a firing cascade. Define EE as the corresponding update matrix for excitatory population after an excitatory firing, while EI as the matrix for inhibitory population after an excitatory firing. Similarly, IE is the matrix for updating excitatory population after an inhibitory firing. Therefore, excitatory and inhibitory firings can be expressed as these updating schemes, $X_E^{new} = EE * X_E$, $X_I^{new} = EI * X_I$; $X_E^{new} = IE * X_E$, respectively. By let entering and exiting condition for a cascade be the same as $(FC)t$ and Section 3.2.4, we complete the descriptions.

C Pesudo-Code of Discrete Mean-Field Formulations

Algorithm 2 Simulating Neural Networks with Leaking and Shunting Inhibitions

$t \leftarrow 0$
Initialize EE, EI, and IE matrices (Section B)
Choose $X_E, X_I \in \mathbb{R}^{+(d+2)}$ such that $\|X_E\|_{l_1} = n_e$ and $\|X_I\|_{l_1} = n_i$ (Section B)
while $t < t_{max}$ **do**
  solve system of ODE's (25)-(30) until $t = t_n$
  $Q \leftarrow [1]$, $total_e = 0$, $total_i = 0$
  while $|Q| > 0$ **do**
    $cur \leftarrow Q(1)$, $newlist \leftarrow [\,]$, $Q \leftarrow Q(2 : end)$
    if $cur = 1$ **then**
      $total_e = total_e + 1$
      $X_E^{new} = EE * X_E$, $X_I^{new} = EI * X_I$
      $\Delta f_e = \lfloor X_E^{new}(d+1) - X_E(d+1) \rfloor$, $\Delta f_i = \lfloor X_I^{new}(d+1) - X_I(d+1) \rfloor$
      randomly generate $newlist$ with Δf_e's 1 and Δf_i's 0
      $X_E = X_E^{new}$, $X_I = X_I^{new}$
    else
      $total_i = total_i + 1$
      $X_E = IE * X_E$
    end if
  end while
  $X_E(d+1) = X_E(d+1) - total_e$, $X_E(d) = X_E(d) + total_e$
  $X_I(d+1) = X_I(d+1) - total_e$, $X_I(d) = X_I(d) + total_e$
end while

References

[1] Abbott, L. and van Vreeswijk, C. (1993). Asynchronous states in networks of pulse-coupled oscillators. *Physical Review E*, 48(2):1483.

[2] Bressloff, P. and Coombes, S. (1998). Desynchronization, mode locking, and bursting in strongly coupled integrate-and-fire oscillators. *Physical Review Letters*, 81(10):2168.

[3] Campbell, S. R., Wang, D. L., and Jayaprakash, C. (1999). Synchrony and desynchrony in integrate-and-fire oscillators. *Neural computation*, 11(7):1595–1619.

[4] DeVille, L. and Zeng, Y. (2014). Synchrony and periodicity in excitable neural networks with multiple subpopulations. *SIAM Journal on Applied Dynamical Systems*, 13(3):1060–1081.

[5] DeVille, R. E. L. and Peskin, C. S. (2008). Synchrony and asynchrony in a fully stochastic neural network. *Bulletin of Mathematical Biology*, 70(6):1608–1633.

[6] Ermentrout, G. B. and Kopell, N. (1984). Frequency plateaus in a chain of weakly coupled oscillators, i. *SIAM journal on Mathematical Analysis*, 15(2):215–237.

[7] Georgiadis, D. and Sornette, D. (2019). Pattern phase diagram of spiking neurons on spatial networks. *Phys. Rev. E*, 99:042410.

[8] Gerstner, W. and van Hemmen, J. L. (1993). Coherence and incoherence in a globally coupled ensemble of pulse-emitting units. *Physical review letters*, 71(3):312.

[9] Hansel, D., Mato, G., and Meunier, C. (1993). Clustering and slow switching in globally coupled phase oscillators. *Physical Review E*, 48(5):3470.

[10] Huygens, C. (2003). Horoloquium oscilatorium. *Parisiis, Paris*, 1673.

[11] Knight, B. W. (1972). Dynamics of encoding in a population of neurons. *The Journal of general physiology*, 59(6):734–766.

[12] Kuramoto, Y. (1991). Collective synchronization of pulse-coupled oscillators and excitable units. *Physica D: Nonlinear Phenomena*, 50(1):15–30.

[13] Kuramoto, Y. (2003). *Chemical oscillations, waves, and turbulence*. Courier Corporation.

[14] Lindner, B., Garcıa-Ojalvo, J., Neiman, A., and Schimansky-Geier, L. (2004). Effects of noise in excitable systems. *Physics reports*, 392(6):321–424.

[15] Mirollo, R. E. and Strogatz, S. H. (1990). Synchronization of pulse-coupled biological oscillators. *SIAM Journal on Applied Mathematics*, 50(6):1645–1662.

[16] Peskin, C. S. (1975). Mathematical aspects of heart physiology. *Courant Inst. Math.*

[17] Pikovsky, A., Rosenblum, M., Kurths, J., and Kurths, J. (2003). *Synchronization: a universal concept in nonlinear sciences*, volume 12. Cambridge university press.

[18] Strogatz, S. (2004). *Sync: The emerging science of spontaneous order*. Penguin UK.

[19] Terman, D., Kopell, N., and Bose, A. (1998). Dynamics of two mutually coupled slow inhibitory neurons. *Physica D: Nonlinear Phenomena*, 117(1-4):241–275.

[20] Tsodyks, M., Mitkov, I., and Sompolinsky, H. (1993). Pattern of synchrony in inhomogeneous networks of oscillators with pulse interactions. *Physical review letters*, 71(8):1280.

[21] Urbanczik, R. and Senn, W. (2001). Similar nonleaky integrate-and-fire neurons with instantaneous couplings always synchronize. *SIAM Journal On Applied Mathematics*, 61(4):1143–1155.

[22] Van Vreeswijk, C., Abbott, L., and Ermentrout, G. B. (1994). When inhibition not excitation synchronizes neural firing. *Journal of computational neuroscience*, 1(4):313–321.

[23] Winfree, A. T. (2001). *The geometry of biological time*, volume 12. Springer Science & Business Media.